Leveraging Nanoscale Plasmonic Modes to Achieve Reproducible Enhancement of Light

Ryan T. Hill[1], **Jack J. Mock**[2,3], **Yaroslav Urzhumov**[2,3], **David S. Sebba**[4], **Steven J. Oldenburg**[4], **Shiuan-Yeh Chen**[2,5], **Anne A. Lazarides**[1,3,5], **Ashutosh Chilkoti**[1,6], and **David R. Smith**[2,3,*]

[1]Center for Biologically Inspired Materials and Material Systems (CBIMMS), Duke University, Box 90271, Durham, NC, 27708.

[2]Department of Electrical and Computer Engineering, Duke University, Box 90201, Durham, NC, 27708.

[3]Center for Metamaterials and Integrated Plasmonics (CMIP), Duke University, Box 90271, Durham, NC, 27708.

[4]nanoComposix, Inc., 4878 Ronson Ct., Suite K, San Diego, CA, 92111.

[5]Department of Mechanical Engineering and Materials Science, Duke University, Box 90300, Durham, NC, 27708.

[6]Department of Biomedical Engineering, Duke University, Box 90281, Durham, NC, 27708

Abstract

The strongly enhanced and localized optical fields that occur within the gaps between metallic nanostructures can be leveraged for a wide range of functionality in nanophotonic and optical metamaterial applications. Here, we introduce a means of precise control over these nanoscale gaps through the application of a molecular spacer layer that is self-assembled onto a gold film, upon which gold nanoparticles (NPs) are deposited electrostatically. Simulations using a three-dimensional finite element model and measurements from single NPs confirm that the gaps formed by this process, between the NP and the gold film, are highly reproducible transducers of surface-enhanced resonant Raman scattering (SERRS). With a spacer layer of roughly 1.6 nm, all NPs exhibit a strong Raman signal that decays rapidly as the spacer layer is increased.

Keywords

nanophotonics; plasmon resonant nanoparticles; surface-enhanced resonant Raman scattering; gold film; doughnut

---

The investigation of metals for use in guiding and controlling light has accelerated over the past decade, as metals offer a potential route to the nanoscale miniaturization of photonic devices. Though metals exhibit considerably more absorption than do their conventional dielectric counterparts, they nevertheless possess unique properties that can add new capabilities and functionalities to photonic devices. In particular, nano-sized metal structures support localized *plasmon* resonances—or coupled electronic/optical excitations—whose

properties can be controlled by tailoring the size and shape of the NP or through the controlled spacing of several NPs.[1-6] Incident light can interact with plasmon resonances and be localized to subwavelength volumes, where an enhancement of the local fields over the incident field typically occurs. These enhanced, localized fields can be used to drive nonlinearities in molecular systems,[7,8] and have been suggested as the basis for optical metamaterials,[9,10] nano-photonic circuits[11] and devices such as plasmonic lasers,[12-15] mixers[16,17] and transistors.[18]

The largest field enhancements in plasmon resonant nanostructures coincide with the most tightly confined fields. A NP with sharp asperities or corners, for example, can enhance fields by a factor of one hundred or more in the localized, sub-nanometer volumes surrounding the asperities.[19] Similarly, fields can also be strongly localized and enhanced within the sub-nanometer regions between NPs that are spaced within a few nanometers. [9,20-23] For those geometries that yield large enhancements, the exact characteristics of the localized field pattern and the enhancement ratio will depend crucially on the sub-nanometer features associated with the NP. The key to unlocking the potential of plasmonic structures is to pattern or control these features at the sub-nanometer scale. While nano-technology has provided us with powerful approaches to nanoscale patterning through lithographic and self-assembly techniques, the control over sub-nanometer feature sizes required to reliably achieve the strongest field enhancements has remained elusive.

A well known phenomenon associated with plasmonic field-enhancements is that of surface enhanced Raman scattering (SERS), in which the inelastic scattering from the vibrational modes of a molecule near a plasmon resonant structure is enhanced by many orders of magnitude. It is universally found that the commonly used roughened films and colloidal NP suspensions generate only a small percentage of 'hot' spots[24,25] from which Raman signals can be detected. Thus, while SERS can be easily demonstrated in bulk solutions and substrates, chip-scale devices or even nano-sized SERS based sensors have been impractical to implement due to the typically low yield in generating the SERS active nanostructure.

The search for improved and consistently reliable SERS substrates with uniformly large field enhancements has resulted in both the fabrication of asymmetric NPs as well as the controlled formation of NP clusters. In the latter case, structures have been created by a number of techniques, including patterning by electron beam or by nanosphere lithography;[26-28] assembly of plasmonic nanostructures in solution using biochemical linkages;[29-31] or control of the relative position of plasmonic nanostructures using atomic force microscopy. [32] Measurements from samples produced by all of these techniques have confirmed the sensitivity of the field enhancement to the dimensions of the gap between the coupled plasmonic surfaces. Yet, none of these techniques has to date, provided sufficient control over the gap dimensions to render any of the fabricated substrates robust enough to reliably support the largest field enhancements.

While the reproducible formation of "real" particle pairs or clusters with controlled sub-nanometer spacing remains a challenging task, the interaction between a NP and its effective image formed in a nearby conducting film (Figure 1A) provides a conceptually orthogonal approach to generate a well defined enhancement region. The spacing between a NP and its image can be controlled by the self-assembly of an insulating, nanoscale thin film onto the metal layer. Metal NPs deposited onto the film can thus have a fixed and highly uniform spacing relative to the metal surface, and hence to their images. The motivation behind this study is to clarify the contribution of the gap dependent enhancement region to SERS, which has recently been observed from NPs coated with Raman active molecules and deposited on metal films.[33-37]

To illustrate the efficacy of the NP-film system in generating large field enhancements, we analyze the surface enhanced resonant Raman scattering (SERRS) from dye coated NPs. Using a fluorescent molecule enables single NP SERRS spectra to be acquired, since the electronic resonance associated with the absorption peak provides a scattering cross-section enhancement of many orders of magnitude in addition to the electromagnetic enhancement. The resonant scattering from dye molecules is sufficiently strong that SERRS spectra are obtainable from just a few or even single molecules; thus, resonant dye molecules can serve as efficient probes of nanoscale enhancement. For the experiments presented here, we used malachite green isothiocyanate (MGITC), a fluorophore whose absorbance peak is in the red portion of the visible spectrum,[38] roughly overlapping with the plasmon resonance of the gold NP-film system and the excitation wavelength.

The reproducibility of this system is due to every NP at a given NP-film spacer, in principle, generating the same field enhancement in the region of the gap, with polarization and other properties identical among all NPs. Figure 1B provides an illustration of the method we employ whereby a 60 nm MGITC coated gold NP is separated from a 45 nm gold film using a single self-assembled molecular layer of poly(allylamine hydrochloride) (PAH, ~0.6 nm). When viewed through a microscope (0.9 NA 100x objective, Figure 1C, left), elastic scattering from film-coupled NPs produce "doughnut" shaped point-spread-functions (PSFs) due to the cancellation of the horizontal dipolar response of the NPs and their images.[39] The uniformity of the PSFs from a collection of NPs within a field of view, as well as the similarity in their intensities and color, provides an indication that the spacing from the film is similar for all NPs. Further confirming the posited orientation of the gap region and the polarized nature of the resonance, it is found that both the elastic scattering and the SERRS intensity from the NP-film system do not respond in any significant way to S-polarized excitation.[38]

The NP-film resonance can be driven either by an incident beam brought in from above the substrate in darkfield illumination (DF: incidence angle 75 degrees from normal); or from below the substrate, using the total internal reflection (TIR: 45 degrees) occurring at the interface to the glass slide substrate.[38] Laser scattering from NPs and SERRS emission from the MGITC molecules within the NP-film gaps was collected by an optical microscope. When the laser scattering image (Figure 1C, left) is compared to the SERRS image (Figure 1C, right), we see that every NP-Film gap acts as an efficient and localized transmitter of SERRS from MGITC into the far field. Also, in most cases the doughnut shaped PSF is observed from the single NP-film SERRS, indicating transmission through the vertically oriented dipole. Figure 1D shows a representative SERRS spectrum acquired from a single film-coupled NP, selected using an adjustable image plane pinhole aperture and relayed to a spectrometer. Distinct resonances corresponding to a collection of vibrational modes specific to the MGITC molecule can be readily identified.[40]

The qualitative understanding of the field enhancing film-coupled NP system provided by an image dipole model is complicated by the imperfection of the image. Therefore, a three-dimensional model using COMSOL Multiphysics, a commercial finite-element mode solver, was constructed to gain a more quantitative understanding of the NP-film system and to enable parametric studies. The exact material properties of the NP, film, spacer layer; and the excitation of surface plasmons in the film were incorporated into a full wave simulation model, which enabled visualization of the near field patterns; collection of the far-field scattered light; and generation of quantitative values for the expected enhancement factors and resonance frequency shifts as a function of parameters of interest, such as incident illumination conditions and NP-film gap distances.

The intensity and color of DF images of elastically scattered white light from a gold NP spaced from a gold film by layer-by-layer deposition of polyelectrolyte (PE) spacer layers[38] (Figure 2A) correlates well with the simulated spectral shift from the model (Figure 2C) and also previously reported[39,41-43] blue shift in the plasmon resonance with increased NP-film spacer distance. A more detailed comparison of the simulated scattering curves with both the measured extinction curves and the measured single NP scattering curves are included in the Supporting Information.

The calculated spatial distribution of the field enhancement at the 633 nm excitation wavelength in the gap region between the NP and its image is shown in Figure 2B. A tighter confinement of the fields within the gap as well as a much greater enhancement of the fields at smaller NP-film gap distances is predicted. At the 1.7 nm gap distance, the volume of the enhancement region is calculated to be ~ 1 nm^3, which would fit up to 5 MGITC molecules. [38] While the majority of signal is likely to originate from just a few molecules, to estimate the total SERRS enhancement, the E^4 field occupying the region within a shell of 2 nm thickness around the surface of the spherical NP is averaged and normalized by the incident field. The 2 nm shell is selected to completely include the ~1 nm thickness of a monolayer of MGITC molecules on a gold surface.[44] The calculated values, plotted on a log scale in Figure 2D, show a non-linear increase with decreasing NP-film gap distance. As the gap narrows, the SERRS signal should climb dramatically.

Experimentally, MGITC SERRS was measured as a function of the NP-film gap dimension by statistically analyzing the total SERRS emission (using DF excitation[38]) from single NPs at each PE spacer distance. The integrated CCD intensities of 20 NPs for each sample were averaged and plotted against NP-film gap distance (Figure 3A). Single diffraction limited scatterers were selected for analysis to eliminate any potential enhanced field contributions from aggregated NPs. The averaged SERRS intensities exhibit a trend as a function of the gap distance that is in good agreement with simulated near-field values. The increased variance of the SERRS intensity at higher field values is attributed primarily to deviations in the physical position of each NP on the polyelectrolyte film and fluctuations in the number of MGITC molecules in the field-enhanced region. Slight variations in either will have a significant effect on the enhancement when the gap is on the order of a few nanometers or smaller.

SERRS spectra and SERRS images from single NPs at each PE layer thickness using P-polarized TIR excitation is shown in Figure 3B. Both MGITC SERRS intensity and spectral resolution are highest at the smallest NP-film gap dimension, highlighting the importance of the control over gap distance for maximizing SERRS signal and information content.

In conclusion, the single particle measurements and simulations presented in this report illustrate the sensitivity of the scattering properties and SERRS enhancements associated with the precise positioning of plasmonic structures. As just one example that demonstrates the value in defining the sub-nanometer architecture of plasmonic NP systems by a simple and tractable approach, reproducible control over the enhancement regions provides a mechanism for generating high-yield SERRS substrates with consistent field enhancements. Such techniques will be necessary to successfully transition the exciting and sometimes exotic optical phenomena associated with metals to practical plasmonic or metamaterial devices and components.

Supplementary Material

Refer to Web version on PubMed Central for supplementary material.

Acknowledgments

REFERENCES AND NOTES

1. Gunnarsson L, Rindzevicius T, Prikulis J, Kasemo B, Käll M, Zou S, Schatz G. J. Phys. Chem. B. 2005; 109:1079–1087. [PubMed: 16851063]

2. Mock JJ, Barbic M, Smith DR, Schultz D, Schultz S. J. Chem. Phys. 2002; 116:6755.

3. Orendorff C, Sau T, Murphy C. Small. 2006; 2:636–639. [PubMed: 17193100]

4. Sönnichsen C, Franzl T, Wilk T, von Plessen G, Feldmann J. New Journal of Physics. 2002; 4:93.91–93.98.

5. Su K-H, Wei Q-H, Zhang X, Mock JJ, Smith DR, Schultz S. Nano Lett. 2003; 3:1087–1090.

6. Sundaramurthy A, Crozier K, Kino G, Fromm D, Schuck P, Moerner W. Phys. Rev. B. 2005; 72:165409.

7. Bakker R, Drachev V, Liu Z, Yuan H-K, Pedersen R, Boltasseva A, Chen J, Irudayaraj J, Kildishev A, Shalaev V. New Journal of Physics. 2008; 10:125022.

8. Schmelzeisen M, Zhao Y, Klapper M, Müllen K, Kreiter M. ACS Nano. 2010; 4:3309–3317. [PubMed: 20481545]

9. Fan JA, Wu C, Bao K, Bao J, Bardhan R, Halas NJ, Manoharan VN, Nordlander P, Shvets G, Capasso F. Science. 2010; 328:1135–1138. [PubMed: 20508125]

10. Shalaev V, Cai W, Chettiar U, Yuan H-K, Sarychev A, Drachev V, Kildishev A. Opt. Lett. 2005; 30:3356–3358. [PubMed: 16389830]

11. Engheta N. Science. 2007; 317:1698. [PubMed: 17885123]

12. Noginov MA, Zhu G, Belgrave AM, Bakker R, Shalaev V, Narimanov EE, Stout S, Herz E, Suteewong T, Wiesner U. Nature. 2009; 460:1110–1112. [PubMed: 19684572]

13. Oulton RF, Sorger VJ, Zentgraf T, Ma R-M, Gladden C, Dai L, Bartal G, Zhang X. Nature. 2009; 461:629–632. [PubMed: 19718019]

14. Bergman D, Stockman M. Phys. Rev. Lett. 2003; 90:027402. [PubMed: 12570577]

15. Cubukcu E, Kort E, Crozier K, Capasso F. Appl. Phys. Lett. 2006; 89:093120.

16. Grady NK, Knight MW, Bardhan R, Halas NJ. Nano Lett. 2010; 10:1522–1528. [PubMed: 20353196]

17. Palomba S, Danckwerts M, Novotny L. Journal of Optics A. 2009; 11:114030.

18. Dionne JA, Diest K, Sweatlock LA, Atwater HA. Nano Lett. 2009; 9:897–902. [PubMed: 19170558]

19. Kottmann J, Martin O, Smith D, Schultz S. Chem. Phys. Lett. 2001; 341:1–6.

20. Garcia-Vidal F, Pendry J. Phys. Rev. Lett. 1996; 77:1163–1166. [PubMed: 10063006]

21. Rycenga M, Camargo PHC, Li W, Moran CH, Xia Y. J. Phys. Chem. Lett. 2010; 1:696–703. [PubMed: 20368749]

22. Aubry A, Lei DY, Fernández-Domínguez AI, Sonnefraud Y, Maier SA, Pendry JB. Nano Lett. 2010 10:2574-2579.

23. Xu H, Aizpurua J, Käll M, Apell P. Phys. Rev. E. 2000; 62:4318–4324.

24. Imura K, Okamoto H, Hossain M, Kitajima M. Nano Lett. 2006; 6:2173–2176. [PubMed: 17034078]

25. Xu H, Käll M. ChemPhysChem. 2003; 4:1001–1005. [PubMed: 14562448]

26. Gunnarsson L, Bjerneld E, Xu H, Petronis S, Kasemo B, Käll M. Appl. Phys. Lett. 2001; 78:802–804.

27. Haynes C, Van Duyne R. J. Phys. Chem. B. 2003; 107:7426–7433.

28. Su K-H, Durant S, Steele J, Xiong Y, Sun C, Zhang X. J. Phys. Chem. B. 2006; 110:3964–3968. [PubMed: 16509683]

29. Chen S-Y, Lazarides AA. J. Phys. Chem. C. 2009; 113:12167–12175.

30. Lim D-K, Jeon K-S, Kim HM, Nam J-M, Suh YD. Nature Materials. 2010; 9:60–67.

31. Vlcková B, Moskovits M, Pavel I, Sisková K, Sládková M, Slouf M. Chem. Phys. Lett. 2008; 455:131–134.

32. Sun M, Fang Y, Yang Z, Xu H. Phys. Chem. Chem. Phys. 2009; 11:9412. [PubMed: 19830324]

33. Anderson DJ, Moskovits M. J. Phys. Chem. B. 2006; 110:13722–13727. [PubMed: 16836316]

34. Daniels JK, Chumanov G. J. Phys. Chem. B. 2005; 109:17936–17942. [PubMed: 16853302]

35. Driskell JD, Lipert RJ, Porter MD. J. Phys. Chem. B. 2006; 110:17444–17451. [PubMed: 16942083]

36. Orendorff CJ, Gole A, Sau TK, Murphy CJ. Anal. Chem. 2005; 77:3261–3266. [PubMed: 15889917]

37. Park W-H, Ahn S-H, Kim ZH. ChemPhysChem. 2008; 9:2491–2494. [PubMed: 18937223]

38. See Supporting Information for descriptions of experimental methods and for supporting discussion.

39. Mock JJ, Hill RT, Degiron A, Zauscher S, Chilkoti A, Smith DR. Nano Lett. 2008; 8:2245–2252. [PubMed: 18590340]

40. Nguyen CT, Nguyen JT, Rutledge S, Zhang J, Wang C, Walker GC. Cancer Letters. 2010; 292:91–97. [PubMed: 20042272]

41. Hu M, Ghoshal A, Marquez M, Kik P. J. Phys. Chem. C. 2010; 114:7509–7514.

42. Knight MW, Wu Y, Lassiter JB, Nordlander P, Halas NJ. Nano Lett. 2009; 9:2188–2192. [PubMed: 19361166]

43. Lévêque G, Martin OJF. Optics express. 2006; 14:9971–9981. [PubMed: 19529391]

44. Domke K, Zhang D, Pettinger B. J. Am. Chem. Soc. 2006; 128:14721–14727. [PubMed: 17090060]
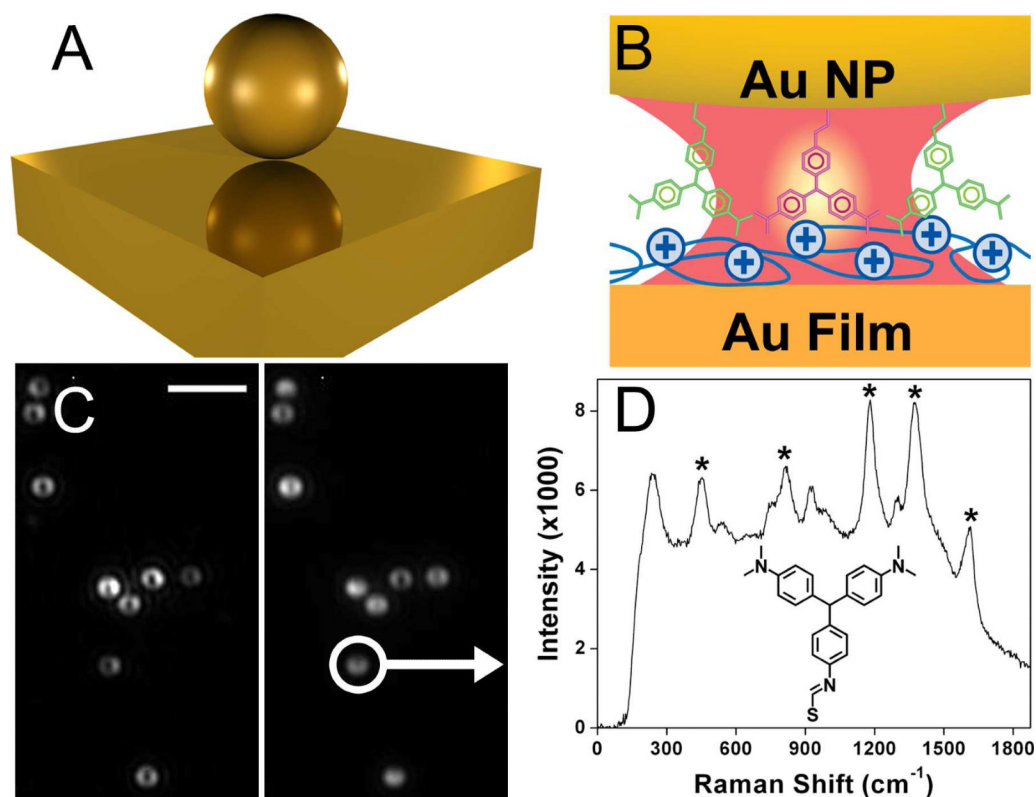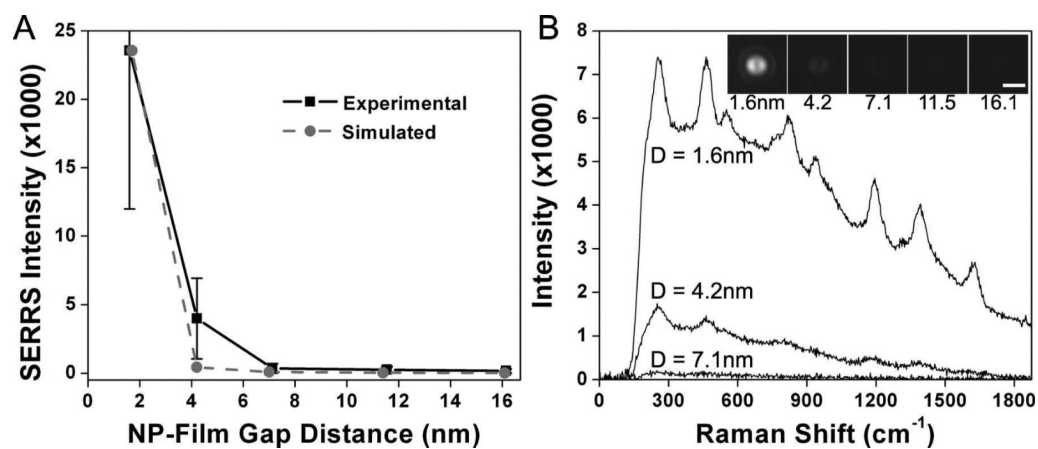
Figure 1.
A gold nanoparticle (NP) near a gold film (A) can be represented as a plasmonically coupled 'dimer' formed between the real NP and its image. B) Localized NP-film field enhancement is used to drive SERRS from MGITC molecules adsorbed on the surface of the NP and within the NP-film gaps, which were created by a single molecular layer of PAH (0.6 nm layer thickness). ~1-5 MGITC molecules are estimated to fit into the enhanced region and contribute to SERRS.[38] C, left) Single NP-film/MGITC resonators elastically scatter TIR incident 633 nm light from a HeNe laser (scale bar = 3μm). C, right) SERRS from the same field was collected by blocking the laser scatter with a long pass filter and was measurable from every single film-coupled NP (100% yield). D) Representative SERRS spectrum collected from a single NP-film gap. The marked lines at 448, 807, 1180, 1370, 1618 relative cm^{-1} are used to identify MGITC.[40]
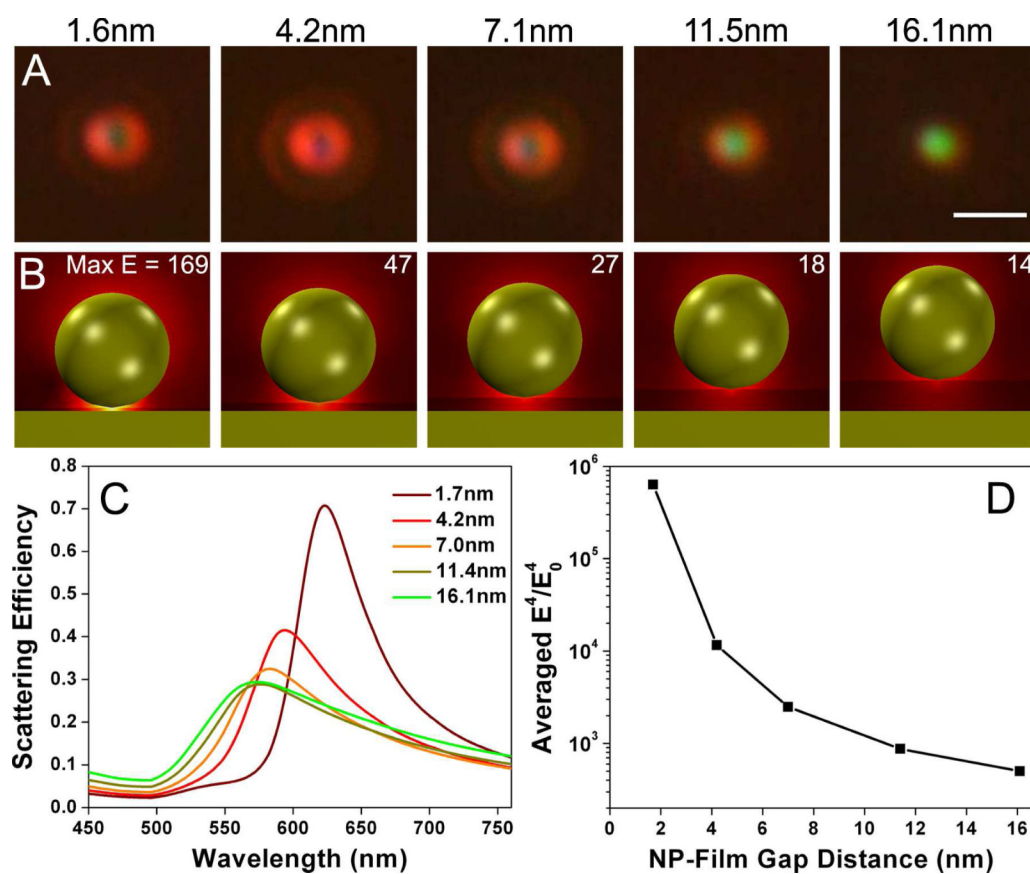
Figure 2.
A) Images of elastic scattering from NPs (DF white light illumination) separated from gold support film by increasing PE spacer distances (scale bar = 1 μm). B) Calculated spatial distribution of the E field (DF illumination, 633 nm) at various gap distances where Max E is the numerical value representing the highest field in each image. C) Calculated scattering efficiency (DF, scattering cross-section integrated over NA = 0.9). D) Averaged E^4/E_0^4 (DF, 633 nm) at various gap distances where E_0 is the amplitude of the incident beam.

Figure 3.
Measured spacer dependence of SERRS from MGITC molecules in the NP-film gaps. A) Averaged SERRS intensities (DF, 633 nm excitation) from 20 NPs (black squares) compared with normalized values of the field enhancement predicted by simulations (data from Figure 2D, plotted again here in A, grey circles). B) Representative MGITC SERRS spectra (TIR, 633 nm excitation) and inset: MGITC SERRS images (scale bar = 1 μm) from single film coupled NPs at increasing gap distance.